SLX4 Assembles a Telomere Maintenance Toolkit by Bridging Multiple Endonucleases with Telomeres

Bingbing Wan,[1,2,3,4,9] Jinhu Yin,[5,9] Kent Horvath,[5,6,9] Jaya Sarkar,[5] Yong Chen,[1,2] Jian Wu,[1,2] Ke Wan,[3,4] Jian Lu,[5] Peili Gu,[7] Eun Young Yu,[8] Neal F. Lue,[8] Sandy Chang,[7] Yie Liu,[5,9,*] and Ming Lei[1,2,3,4,9,*]

[1]State Key Laboratory of Molecular Biology, Institute of Biochemistry and Cell Biology, Shanghai Institutes for Biological Sciences, Chinese Academy of Sciences, 320 Yueyang Road, Shanghai 200031, China
[2]National Center for Protein Science Shanghai, Institute of Biochemistry and Cell Biology, Shanghai Institutes for Biological Sciences, Chinese Academy of Sciences, 320 Yueyang Road, Shanghai 200031, China
[3]Howard Hughes Medical Institute, University of Michigan Medical School, 1150 W. Medical Center Drive, Ann Arbor, MI 48109, USA
[4]Department of Biological Chemistry, University of Michigan Medical School, 1150 W. Medical Center Drive, Ann Arbor, MI 48109, USA
[5]Laboratory of Molecular Gerontology, National Institute on Aging/National Institute of Health, 251 Bayview Drive, Baltimore, MD 21044, USA
[6]Graduate School of Biomedical Sciences at New Jersey Medical School, 185 South Orange Avenue, Newark, NJ 07103, USA
[7]Department of Laboratory Medicine and Pathology, Yale University School of Medicine, 330 Cedar Street, New Haven, CT 06520, USA
[8]Department of Microbiology and Immunology, W. R. Hearst Microbiology Research Center, Weill Medical College of Cornell University, New York, NY 10065, USA
[9]These authors contributed equally to this work
*Correspondence: liuyie@mail.nih.gov (Y.L.), leim@sibcb.ac.cn (M.L.)
http://dx.doi.org/10.1016/j.celrep.2013.08.017

SUMMARY

SLX4 interacts with several endonucleases to resolve structural barriers in DNA metabolism. SLX4 also interacts with telomeric protein TRF2 in human cells. The molecular mechanism of these interactions at telomeres remains unknown. Here, we report the crystal structure of the TRF2-binding motif of SLX4 (SLX4$_{TBM}$) in complex with the TRFH domain of TRF2 (TRF2$_{TRFH}$) and map the interactions of SLX4 with endonucleases SLX1, XPF, and MUS81. TRF2 recognizes a unique HxLxP motif on SLX4 via the peptide-binding site in its TRFH domain. Telomeric localization of SLX4 and associated nucleases depend on the SLX4-endonuclease and SLX4-TRF2 interactions and the protein levels of SLX4 and TRF2. SLX4 assembles an endonuclease toolkit that negatively regulates telomere length via SLX1-catalyzed nucleolytic resolution of telomere DNA structures. We propose that the SLX4-TRF2 complex serves as a double-layer scaffold bridging multiple endonucleases with telomeres for recombination-based telomere maintenance.

INTRODUCTION

Telomeres are highly conserved chromosome end structures, composed of the shelterin protein complex and a double-stranded tract of tandem repeats that ends in a single-stranded 3'-overhang of the G-strand in mammals (Blackburn, 2001). The 3' single-stranded overhang has been proposed to invade the duplex region of telomeric DNAs, base-pairing with the C-strand, forming a "t-loop" configuration (Griffith et al., 1999). Shelterin consists of several proteins including duplex telomeric DNA-binding proteins TRF1 and TRF2 that anchor shelterin along the telomere repeats (Palm and de Lange, 2008). TRF1 and TRF2 are also the principle mediators that recruit many nonshelterin telomere accessory proteins including Apollo (Palm and de Lange, 2008) to telomeres (Palm and de Lange, 2008). The telomere restriction fragment homology (TRFH) domains of TRF1 and TRF2 (Li et al., 2000) directly recognize specific but distinct motifs on their interacting proteins (Chen et al., 2008).

A critical aspect of telomere maintenance is telomere length homeostasis, involving telomerase-catalyzed extension and alternative lengthening of telomeres (ALT). In addition, TRF1 and TRF2 are negative regulators of telomere length (Ancelin et al., 2002; Smogorzewska et al., 2000; van Steensel and de Lange, 1997). Although TRF1 is believed to regulate telomerase in cis at individual telomeres, TRF2 may control telomere length by telomere degradation (Ancelin et al., 2002). Homologous-recombination (HR)-mediated resolution of t-loop has also been proposed to be the underlying mechanism for a negative telomere length regulation process, referred to as "telomere trimming" (Pickett et al., 2009; Wang et al., 2004), which leads to deletion of large telomeric segments that are detectable as extrachromosomal telomeric circles (TCs) (Pickett et al., 2009, 2011; Wang et al., 2004). Some cancer cells maintaining telomere length via ALT exhibit abundant TCs (Henson and Reddel, 2010) and likely utilize telomere trimming to counteract HR-mediated telomere lengthening (Cesare and Reddel, 2010). Yet, the regulatory mechanism for telomere trimming is not fully understood.

A Fanconi anemia (FA) protein, SLX4 (or BTBD12 or FANCP), is a molecular scaffold that interacts with structure-specific

endonucleases XPF-ERCC1, MUS81-EME1, and SLX1 (Fekairi et al., 2009; Kim et al., 2013; Muñoz et al., 2009; Svendsen et al., 2009). SLX4 also associates with TRF2 in human cells (Svendsen et al., 2009). However, the nature of this interaction and the functional significance of SLX4 at telomeres remain unknown. Here, we report that telomeric localization of SLX4 and its associated nucleases depends on the interaction between a unique HxLxP motif of SLX4 and the TRFH domain of TRF2. We propose that SLX4 together with TRF2 forms a double-layer scaffold that assembles a telomere maintenance toolkit, containing XPF, MUS81, and SLX1, where the SLX4-SLX1 module regulates telomere length via SLX1-catalyzed resolution of telomeric DNA structures.

RESULTS

Telomeric Localization of SLX4 Depends on Protein Levels of SLX4 and TRF2

To investigate the involvement of SLX4 in telomere maintenance, we examined telomeric localization of endogenous SLX4 in different human cell lines, including telomerase-negative ALT cells (U2OS, WI38[VA13-2RA], and GM847), telomerase-positive cancer cells (HT1080, HeLa, and its subclone HeLa1.2.11), and primary cells (BJ and MRC5). Indirect immunofluorescence (IF) showed that SLX4 formed discrete nuclear foci in all of these cells (Figures 1A and S1A; data not shown). Unlike the primary (BJ) and telomerase-positive (HT1080 and HeLa) cancer cells, the majority of the SLX4 foci in ALT and HeLa1.2.11 cells colocalized with TRF2 and telomeres (Figures 1A and S1A). The association of SLX4 with telomeres in U2OS and HeLa1.2.11 cells was also confirmed by chromatin immunoprecipitation (ChIP) (Figure S1B). Because telomeres in ALT cells are substantially longer than those in other cells and HeLa1.2.11 cells possess longer telomeres than its parental HeLa cells (Figure 1B), we reasoned that SLX4 may preferentially localize to longer telomeres. Indeed, SLX4 increasingly localized to telomeres in telomerase-positive cells with longer telomeres (Figures 1C and 1D; Supplemental Information). Notably, the few telomeres in the ALT (U2OS) cells that did not colocalize with SLX4 foci also exhibited substantially weaker signals than the majority of SLX4-overlapping telomeres (Figure 1E), further suggesting that SLX4 tends to be targeted to longer telomeres. The amount of SLX4 at individual telomeres was also dependent on the protein levels of SLX4 and TRF2 (Figures 1F and S1C; Supplemental Information), which in many cells positively correlate with longer telomere length.

A Short Motif on SLX4 Mediates the SLX4-TRF2 Interaction Essential for Telomeric Localization of SLX4

TRF2 interacts with the middle region of SLX4 (Svendsen et al., 2009). We found that SLX4 binds to the TRFH domain of TRF2 (TRF2$_{TRFH}$) by yeast two-hybrid (Y2H) assay (data not shown). Various fragments of SLX4 were evaluated for their ability to interact with TRF2$_{TRFH}$ by Y2H and isothermal titration calorimetry (ITC) assays (Figures S2A–S2E). A short fragment of SLX4 consisting of residues 1014–1028 (SLX4$_{1014-1028}$) was sufficient for binding with TRF2$_{TRFH}$ with a K_D of 750 nM (Figures 2A and 2B), whereas binding enthalpy between SLX4$_{1014-1028}$ and TRF1$_{TRFH}$ was not measurable by ITC (Figure S2F), indicating

that SLX4$_{1014-1028}$ binding is specific for TRF2. We hereafter refer to SLX4$_{1014-1028}$ as SLX4$_{TBM}$ (TRF2-binding motif) (Figure 2A).

We have demonstrated that TRF2$_{TRFH}$ specifically recognizes a short peptide motif with a signature sequence YxLxP (x: any amino acid) on its interacting proteins including Apollo (Chen et al., 2008). SLX4$_{TBM}$ contains a modified sequence HxLxP (Figure 2A) that highly resembles the TRF2$_{TRFH}$ binding motif of Apollo (Apollo$_{TBM}$) (Figure 2A) (Chen et al., 2008), suggesting that SLX4$_{TBM}$ might bind to TRF2$_{TRFH}$ in the same fashion as Apollo$_{TBM}$. We solved the crystal structure of the TRF2$_{TRFH}$-SLX4$_{TBM}$ complex at 2.05 Å resolution (Figure S2G; Table S1). The structure exhibits a 2:2 stoichiometry between TRF2$_{TRFH}$ and SLX4$_{TBM}$. Each SLX4$_{TBM}$ peptide adopts an extended conformation with a short one-turn helix at the N terminus and fits into the narrow groove formed by TRF2$_{TRFH}$ (Figure 2C). Except for the very N terminus, SLX4$_{TBM}$ and Apollo$_{TBM}$ are identical in overall conformation (Figure 2D). Two key hydrophobic residues in SLX4$_{TBM}$, L1022, and P1024 bind to TRF2$_{TRFH}$ in the same fashion as do their counterparts in Apollo$_{TBM}$. The imidazole ring of SLX4 H1020 occupies the same position as the side chain of Apollo Y504 in the Apollo$_{TBM}$-TRF2$_{TRFH}$ complex (Figure 2D) (Chen et al., 2008).

To investigate the importance of the interface residues of SLX4$_{TBM}$ or TRF2$_{TRFH}$ in the SLX4-TRF2 interaction, we focused on four hydrophobic residues: F120 of TRF2 and H1020, L1022, and P1024 of SLX4, whose equivalents in other TRF2$_{TRFH}$-binding proteins are critical for their respective interactions (Chen et al., 2008). ITC data showed that alanine substitutions of these residues either completely abolished (SLX4 L1022A and TRF2 F120A) or substantially impaired (SLX4 H1020A and P1024A) the SLX4-TRF2 interaction (Figures 2E, S2H, and S2I). Consistent with the ITC analysis, coimmunoprecipitation (co-IP) revealed that while SLX4$_{L1022A}$ and TRF2$_{F120A}$ completely disrupted the association between SLX4 and TRF2, mutations of SLX4 H1020 and P1024 to alanine retained weak interactions with TRF2 in human embryonic kidney 293T cells (Figure 2F). Furthermore, SLX4$_{L1022A}$ was efficiently coimmunoprecipitated with MUS81 (Figure 2F) that is known to bind to the C-terminal region of SLX4 (Fekairi et al., 2009; Kim et al., 2013; Svendsen et al., 2009). Hence, the observed SLX4-TRF2 interface is specific and necessary for both in vitro and in vivo binding of SLX4 to TRF2.

We tested the relevance of the SLX4-TRF2 interaction to the telomeric localization of SLX4 in U2OS and HeLa1.2.11 cells transiently expressing wild-type (WT) or mutant GFP-SLX4 fusion protein and HA-tagged WT or mutant TRF2. IF analysis revealed a nuclear punctate staining pattern for WT SLX4 that almost completely colocalized with TRF2 (Figures 2G and S2J–S2L). In contrast, the SLX4$_{L120A}$ and TRF2$_{F120A}$ mutants disrupted the colocalization of SLX4 and TRF2 (Figures 2G and S2J–S2L). As both WT TRF2 and TRF2$_{F120A}$ mutant can efficiently localize to telomeres (Figures 2G and S2J–S2L), these results demonstrate that SLX4 binding to TRF2$_{TRFH}$ is required for telomeric localization of SLX4.

Nuclear Foci Formation and Telomeric Localization of XPF, MUS81, and SLX1 Are Mediated by SLX4

SLX4 contains modules that interact with other protein factors, including XPF, MUS81, and SLX1 (Fekairi et al., 2009; Kim
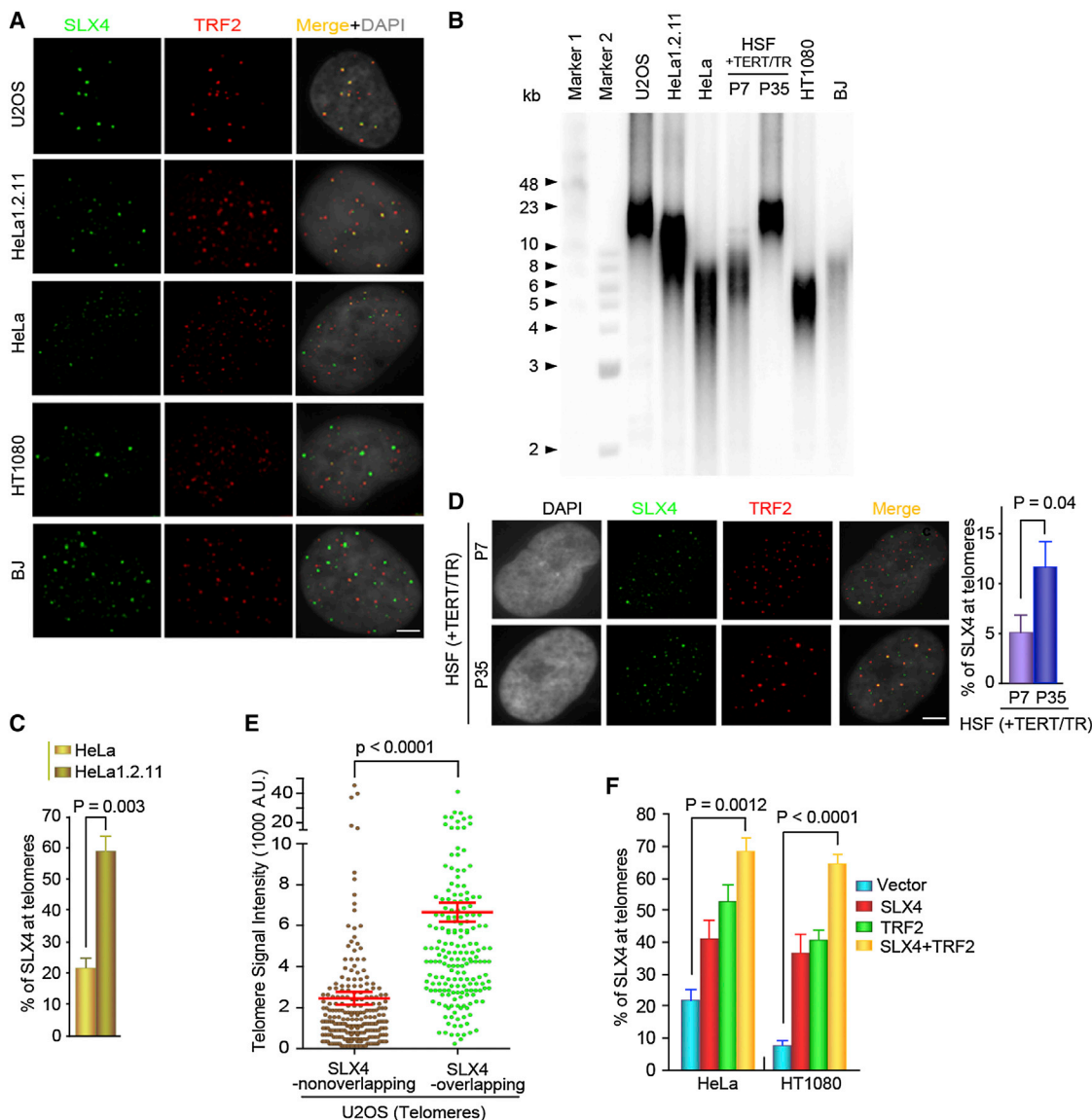
Figure 1. Association of SLX4 with Telomeres Is Dependent on Proteins Levels of SLX4 and/or TRF2

(A) Endogenous SLX4 and TRF2 colocalization in human cells. Bar: 5 μm.

(B) Telomere length in different human cell lines by TRF analysis.

(C) Percentage of SLX4 foci at telomeres in HeLa and HeLa1.2.11 cells. One hundred cells/genotype were examined. p value: two-tailed Student's test.

(D) Telomeric localization of SLX4 in primary human fibroblasts induced with hTERT and hTR (long telomeres: HSF-P35; short telomeres: HSF-P7). Error bars: SD; p values: two-tailed Student's t test.

(E) Signal intensity of SLX4-nonoverlapping or -overlapping telomeres. Error bars: SD. p values: two-tailed Student's t test.

(F) Percentage of SLX4 foci at telomeres in HeLa and HT1080 cells transfected with SLX4 and/or TRF2. Error bars: SD; p values: two-tailed Student's t test.

See also Figure S1.

et al., 2013; Muñoz et al., 2009; Svendsen et al., 2009). Using Y2H assay, we mapped three nonoverlapping fragments of SLX4 that interact with XPF, MUS81, and SLX1 (Figures 3A and S3A–S3C), hereafter referred to as XBR (*X*PF-*b*inding *r*egion), MBR (*M*US81-*b*inding *r*egion), and SBR (*S*LX1-*b*inding *r*egion), respectively (Figure 3A). Co-IP showed that the deletion mutants of SLX4 (SLX4$_{\Delta XBR}$, SLX4$_{\Delta MBR}$, and SLX4$_{\Delta SBR}$), each lacking only the specific interacting region for one endonuclease,

specifically abolished only the targeted interaction in cells (Figure 3B). Furthermore, IF analysis demonstrated that nuclear foci formation of XPF, MUS81, and SLX1 relied on their specific interactions with SLX4 (Figures 3C and S3D–S3F; Supplemental Information).

Because TRF2 bridges SLX4 with telomeres, we tested whether the SLX4-TRF2 interaction is critical for telomeric localization of the SLX4-interacting nucleases. We utilized either the
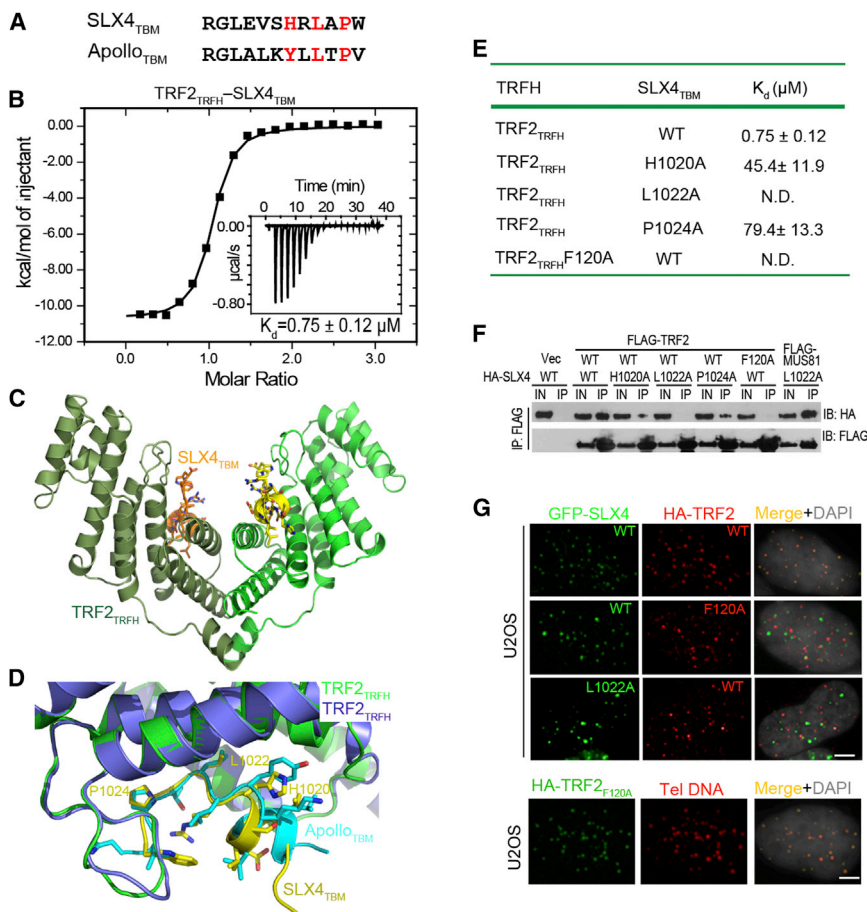
SLX4 in T-SCE. Expression of WT SLX4 (Figure S4C) elevated the level of T-SCEs to ~0.45 T-SCEs/chromosome, thereby rescuing the defect in T-SCE caused by SLX4 depletion (Figure S4G). In contrast, expression of the TRF2-binding-deficient SLX4$_{L1022A}$ (Figure S4C)

SLX4$_{L1022A}$ or the TRF2$_{F120A}$ mutant, each of which can independently abolish the SLX4-TRF2 interaction (Figures 2E–2G and S2H–S2L), and individually expressed each endonuclease with SLX4$_{L1022A}$ (Figures 3E and S3G) or TRF2$_{F120A}$ (data not shown) and assayed their nuclear localization. Although XPF, MUS81, and SLX1 formed discrete foci that colocalized with SLX4$_{L1022A}$, they failed to be targeted to telomeres (Figures 3E and S3G). Also, all three nucleases failed to colocalize with TRF2$_{F120A}$ (data not shown). Hence, SLX4 functions as a scaffold to target XPF, MUS81, and SLX1 to telomeres via its interaction with TRF2.

SLX4 Mediates Its Affiliated Nucleases in Regulating Telomere Recombination

MUS81 has been shown to regulate T-SCE in human ALT cells (Zeng et al., 2009). Because the telomeric localization of MUS81 depends on SLX4 (Figure 3C), we asked whether SLX4 is required for telomere recombination. We depleted SLX4 in U2OS cells using small hairpin RNA (shRNA) (Figures S4A–S4C) and analyzed T-SCE by chromosome orientation (CO) fluorescence in situ hybridization (FISH) (Figures S4D and S4E). Whereas U2OS cells exhibited ~0.2 T-SCEs/chromosome, depletion of SLX4 decreased the frequency to ~0.04 T-SCEs/chromosome (Figure S4F), underscoring the importance of

failed to fully promote T-SCE (Figure S4G), suggesting that telomeric localization of SLX4 is crucial for T-SCE.

Because XPF, MUS81, and SLX1 are recruited to telomeres by SLX4, we examined the role of each of these endonucleases in T-SCE by expressing SLX4$_{\Delta XBR}$, SLX4$_{\Delta MBR}$, or SLX4$_{\Delta SBR}$ deletion mutants in SLX4-depleted U2OS cells (Figure S4C). None of these mutants was able to rescue the T-SCE defects due to SLX4 depletion (Figure S4G), indicating that all three endonucleases are required for T-SCE in U2OS cells. Similar results were also observed in HeLa1.2.11 cells (Figure S4H). Thus, SLX4 regulates telomere recombination, which is dependent on the SLX4-TRF2 scaffold and also on the nucleases XPF, MUS81, and SLX1.

SLX4 Negatively Regulates Telomere Length via Association with SLX1

In mammalian cells, telomere length is maintained at or near an equilibrium point. Because SLX4 is preferentially detected at longer telomeres and interacts with nucleases in human cells (Figures 1 and 3), we investigated the role of SLX4 and its associated nucleases in telomere length regulation. U2OS cells stably expressing SLX4 shRNA were transiently transfected with either empty GFP vector or GFP-fused WT or mutant SLX4 and subsequently analyzed for telomere length using quantitative FISH
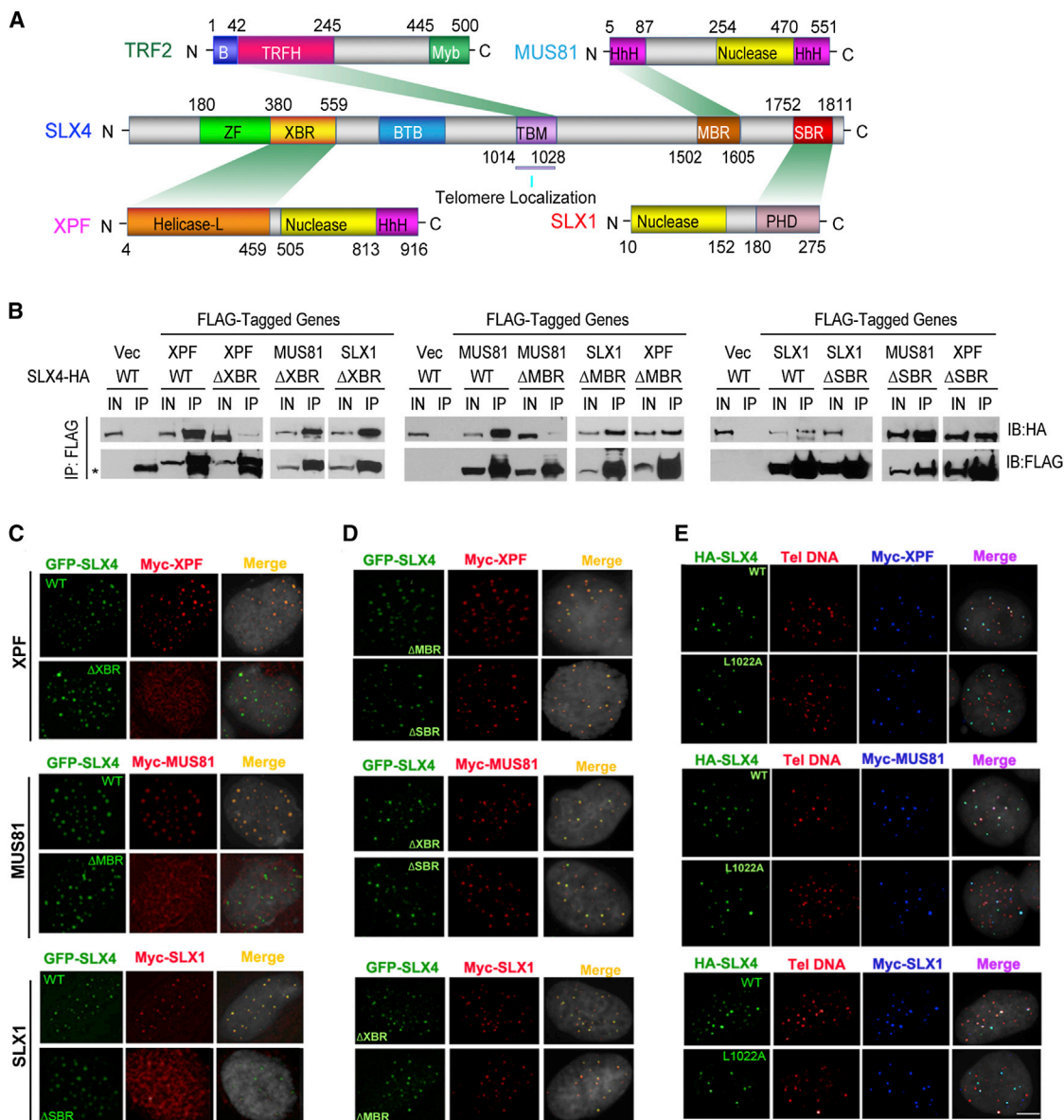
Figure 3. SLX4 Serves as a Scaffold to Assemble a Nuclease Toolkit at Telomeres

(A) Domain organization of SLX4 and its interacting proteins. The shaded areas between SLX4 and its interacting proteins indicate the regions of the respective protein-protein interactions. B, basic domain.

(B) Co-IP confirmation of SLX4-nuclease interacting regions. Lanes marked "IN" contain 5% of the input lysate used for IPs. Asterisk: nonspecific band.

(C and D) IF analysis of foci formation and colocalization of the nucleases in SLX4-depleted U2OS cells expressing WT or deletion mutants of SLX4 that either disrupt (C) or preserve (D) the respective interactions.

(E) IF-telomere FISH analysis of foci formation and colocalization of the nucleases with telomeric DNA in SLX4-depleted U2OS cells expressing WT SLX4 or TRF2-binding-deficient mutant $SLX4_{L1022A}$.

See also Figure S3.

(Q-FISH) analysis. SLX4-depleted cells (vec) exhibited a 2-fold increase in telomere length in comparison to the control cells (Scramble) (Figures 4A, S5A, and S5B), indicating that SLX4 is a negative regulator of telomere length. Telomere length was quickly restored to the levels of control cells, 24–48 hr after expression of WT SLX4 (Figure 4A). This suggests that the telomere lengthening in SLX4-depleted cells is attributable to SLX4 deficiency. Expression of the TRF2-binding-deficient mutant $SLX4_{L1022A}$ could not restore telomere length in SLX4-depleted cells to that of control cells (Figure 4A), underscoring the importance of TRF2-mediated telomeric localization of SLX4 in telomere length regulation. Interestingly $SLX4_{\Delta SBR}$ failed to rescue the telomere length defect due to SLX4 depletion, whereas $SLX4_{\Delta XBR}$ or $SLX4_{\Delta MBR}$-expressing cells exhibited normal or a
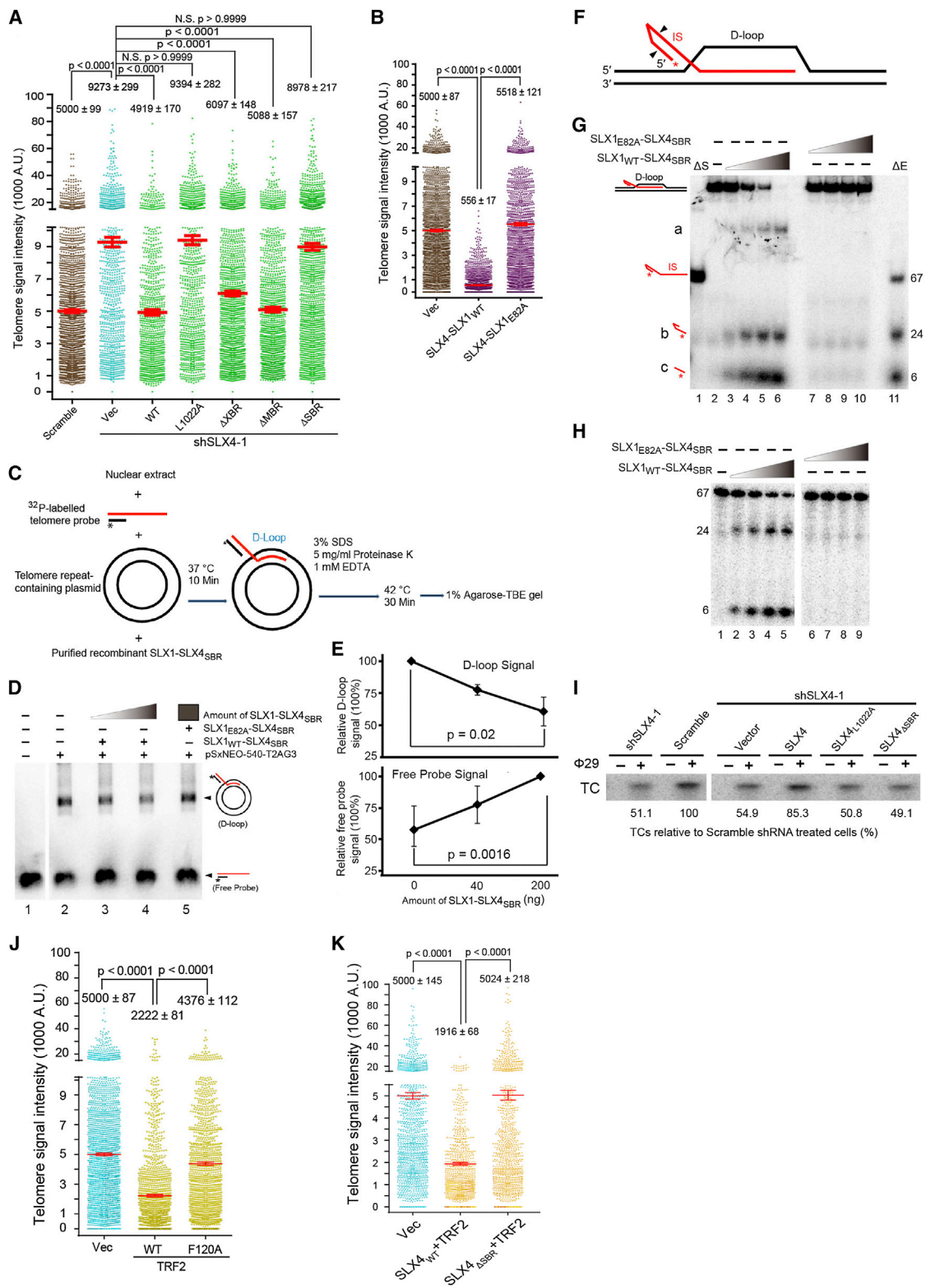
Figure 4. The SLX4-SLX1 Nuclease Complex Regulates Telomere Length and T-Loop Resolution

(A and B) Telomere length in SLX4-depleted U2OS cells expressing WT or mutant SLX4 (A) or WT SLX4 fused to WT or nuclease dead (E82A) mutant of SLX1 (B). Mean telomere length was derived from three independent experiments. NS, nonsignificance. p values: one-way ANOVA.

(C) Plasmid-based D-loop assay in the presence of purified SLX1-SLX4$_{SBR}$ complex.

(legend continued on next page)

slightly longer average length than those in control cells (Scramble) (Figure 4A). These results support that, among the three endonucleases, SLX1 is essential for telomere length regulation in human cells.

To examine whether SLX1 regulates telomere length by nucleolytic cleavage of telomere DNAs, we utilized the nuclease-deficient E82A mutant of SLX1 (SLX1$_{E82A}$). Because SLX1 is neither stable nor active without SLX4 (Svendsen et al., 2009), we generated chimeric constructs expressing WT or E82A SLX1 fused to SLX4, referred to as SLX4-SLX1$_{WT}$ or SLX4-SLX1$_{E82A}$. Expression of SLX4-SLX1$_{WT}$ in SLX4-depleted U2OS cells caused a marked reduction in telomere length as compared to the control cells (vec). In sharp contrast, expression of SLX4-SLX1$_{E82A}$ had no effect on telomere length (Figure 4B). Similar results were observed in HeLa1.2.11 cells (Figure S5C). These data suggest that the nuclease activity of the SLX4-SLX1 complex plays an important role in telomere length maintenance in human cells.

The SLX4-SLX1 Complex Provides Nuclease Activity for T-Loop Resolution

Negative regulation of telomere length in human cells might involve a highly controlled process called "telomere trimming" via nucleolytic resolution of t-loops, leading to formation of TCs (Pickett et al., 2009, 2011; Wang et al., 2004). The SLX4-SLX1 complex displays robust resolution activity towards HJ substrates in vitro (Fekairi et al., 2009; Muñoz et al., 2009; Svendsen et al., 2009) and might mediate negative regulation of telomere length by catalyzing nucleolytic resolution of the t-loop. We first employed a plasmid-based D-loop assay (Verdun and Karlseder, 2006) to examine whether SLX4-SLX1 is capable of resolving D-loop, an intrinsic part of a t-loop, in vitro. In this assay, we relied on the requisite protein factors in nuclear extract to form a D-loop in the presence of a telomeric-repeat-containing plasmid (pSxNeo540-T$_2$AG$_3$) and a radiolabeled telomeric probe, with or without purified recombinant full-length SLX1 in complex with the C-terminal SBR domain of SLX4 (SLX1-SLX4$_{SBR}$) (Figure 4C). With increasing amount of the SLX1$_{WT}$-SLX4$_{SBR}$ complex, the radioactive signal corresponding to the D-loop significantly decreased in intensity, with concomitant increase in free probe intensity, suggesting that the SLX1-SLX4 complex antagonizes or impedes D-loop formation in vitro (Figures 4D and 4E). In contrast, D-loop or free probe signal was unaltered when the catalytically deficient mutant SLX1$_{E82A}$-SLX4$_{SBR}$ complex was added in the assay, even at the maximum concentration (Figures 4D and 4E). Thus, the endonuclease activity of SLX1 is likely instrumental in thwarting D-loop formation.

To gain better mechanistic insight into D-loop resolution by the SLX1-SLX4 complex, we generated a model immobile telomeric D-loop structure in vitro, assembled from oligonucleotides (Figure 4F) (Opresko et al., 2004). A 67-mer invading strand (IS) that mimics the 3′-telomeric overhang was radiolabeled at the 5′ end and hybridized with the melted region of a duplex DNA to form a telomeric D-loop structure. Increasing amounts of the SLX1$_{WT}$-SLX4$_{SBR}$ complex resulted in disappearance of the D-loop substrate and the appearance of three bands (denoted by a, b, c), migrating below the D-loop on a native gel (Figure 4G, lanes 3–6, and Figure S5D). Bands "b" and "c" correspond to the digested and released products of the IS (Figure 4G, compare lanes 3–6 with 11), whereas band "a" very likely represents a partially resolved D-loop that remains associated with the intact IS, formation of which requires nucleolytic cleavage by SLX1, as implied from the absence of this band in the nuclease dead mutant (Figure 4G, compare lanes 3–6 with 7–10). The two cleavage products (b and c) were also visualized by a denaturing gel and are approximately 24-mer and 6-mer in length, respectively (Figure 4H, lanes 2–5). Significantly, in vivo, a nucleolytic cut on the invading 3′-telomeric overhang would predictably result in resolution of the t-loop structure. In contrast, the D-loop substrate was completely resistant to the catalytically deficient SLX1$_{E82A}$-SLX4$_{SBR}$ mutant complex (Figure 4G, lanes 7–10, Figure 4H, lanes 6–9, and Figure S5D). These data support that the endonuclease activity of SLX1 is necessary for the cleavage and release of the IS and hence for proper resolution of the D-loop structure in vitro.

We reasoned that, if the SLX1-SLX4 complex nucleolytically resolves D-loops in vitro, this might translate into enhanced TC formation in vivo. We analyzed TC formation in U2OS cells depleted of SLX4 by employing a Φ29 DNA-polymerase-dependent T-circle amplification (TCA) assay (Figures 4I and S5E) (Zellinger et al., 2007). A substantial decrease in TC formation was observed in SLX4-depleted cells (Figure 4I, shSLX4-1), as compared to control shRNA-treated cells (scramble), suggestive of the importance of SLX4 in TC biogenesis in human cells. TC formation was nearly completely rescued by WT SLX4 but not the SLX1-binding-deficient mutant SLX4$_{\Delta SBR}$ (Figure 4I), further supporting that SLX1 plays an important role in the generation of TCs. We also observed that expression of the TRF2-binding-deficient mutant SLX4$_{L1022A}$ in SLX4-depleted U2OS cells

---

(D and E) Agarose gel (D) and quantification (E) showing SLX1$_{WT}$-SLX4$_{SBR}$ complex-dependent change in radioactive signals corresponding to the D-loop and free probe. For each reaction, the D-loop and free probe signal were normalized to the reactions containing no (0 ng) and maximum enzyme (200 ng), respectively. Lane 1 in (D) denotes the control without telomere repeat-containing plasmid. Error bars denote variations from three independent experiments.

(F) The oligonucleotide-based telomeric D-loop substrate. The invading strand (IS) was labeled with [^{32}P]-γ-ATP at the 5′ end (in red). Arrows: possible cleavage sites by the SLX1-SLX4$_{SBR}$ nuclease complex.

(G and H) The telomeric D-loop substrate was incubated with increasing amounts of the SLX1$_{WT}$-SLX4$_{SBR}$ or SLX1$_{E82A}$-SLX4$_{SBR}$ complexes. The IS and cleavage products are indicated on native (G) or denaturing (H) gel. Symbols ΔS (lane 1): heat denatured substrate alone. ΔE (lane 11): substrate incubated with maximum amount of the WT enzyme complex, followed by heat denaturation.

(I) TCA assay in SLX4-depleted U2OS cells, transiently expressing vector, WT, or mutant SLX4. The TC signal was normalized to the scramble control (lane 2) that was set for 100%.

(J and K) The SLX4-SLX1 complex is a player in TRF2-mediated telomere shortening. Q-FISH analysis of telomere length in U2OS cells expressing WT or mutant TRF2 alone (J) or together with SLX4$_{WT}$ or SLX4$_{\Delta SBR}$ (K). Mean telomere length was derived from three independent experiments. Error Bars: SD. NS, nonsignificance. p values: one-way ANOVA.

See also Figure S5.

failed to rescue TC-formation to control levels, underscoring the importance of SLX4-TRF2 interaction in SLX1-dependent TC formation and is consistent with the colocalization data that targeting SLX1 to telomeres is dependent on the SLX4 and TRF2 interaction (Figure 3E).

TRF2-Mediated Telomere Shortening Relies upon the SLX4-SLX1 Complex

Expression of TRF2 causes rapid loss of telomeres in ALT cells (Figure 4J) (Ancelin et al., 2002). Of note, overexpression of the $TRF2_{F120A}$ mutant did not alter telomere length (Figure 4J), suggesting that factors that bind to the TRFH peptide-binding site of TRF2 contribute to telomere shortening. Because SLX4 interacts with TRF2 via the TRFH peptide-binding site and depletion of SLX4 leads to telomere lengthening (Figure 4A), SLX4 might be required for TRF2-mediated telomere shortening in ALT cells. U2OS cells were cotransfected with mCherry-fused WT TRF2 and GFP-fused WT SLX4 or the SLX1-binding-deficient mutant $SLX4_{\Delta SBR}$. Cells positive for GFP and mCherry signals were analyzed for telomere length by Q-FISH. Coexpression of TRF2 and SLX4 led to rapid telomere loss (Figures 4K). In contrast, coexpressing TRF2 and $SLX4_{\Delta SBR}$ had no detectable effect on telomere length (Figures 4K and S5F). A similar result was also observed in HeLa1.2.11 cells (Figure S5G). Thus, TRF2-mediated rapid telomere shortening requires SLX1 that is recruited to telomeres via SLX4.

For additional details, see the Extended Results.

DISCUSSION

In this report, we provide structural, molecular, and cellular evidence that SLX4 through its interaction with TRF2 functions as a "double-layer scaffold" to organize a multinuclease "telomere maintenance" toolkit. Assembly of this toolkit requires the SLX4-TRF2 interaction and three nonoverlapping motifs of SLX4 (XBR, MBR, and SBR) to recruit endonucleases XPF, MUS81, and SLX1, respectively, to the SLX4 foci. An advantage of this "double-layer" scaffold is that it can more efficiently recruit multiple proteins simultaneously to telomeres with fixed stoichiometry than a "single-layer" architecture in which all factors would be recruited by interactions with TRF2 alone. Another advantage is that SLX4 may function not only as the binding platform for the endonucleases, but also as a coordinator, orchestrating complicated processes at telomeres in a regulated manner. Given that all three endonucleases are required for proper T-SCE and that each nuclease exhibits different in vitro substrate preference (Fekairi et al., 2009; Muñoz et al., 2009; Svendsen et al., 2009), it is likely that T-SCE requires activities of all three nucleases, coordinated by SLX4. In fact, it has been proposed that resolution of HJs in vivo by the SLX4-nuclease complex may require SLX1 to first create a nicked intermediate that is then acted upon by MUS81 (Svendsen et al., 2009).

TRF1 and yeast telomeric protein Rap1 function as *cis*-acting negative regulators of telomere length (Bianchi and Shore, 2008; van Steensel and de Lange, 1997). TRF2 is also a negative regulator of telomere length and its expression causes rapid loss of telomeres in human ALT cells (Ancelin et al., 2002). Here, we unveil the SLX4-SLX1 nuclease complex assembled on telomeres

as a player in TRF2-mediated negative telomere length regulation in *cis* and propose the following model (Figure S5H). TRF2 binds to telomeric DNA and functions as a measuring device to assess telomere length. Longer telomeres are bound by larger amount of TRF2, which subsequently recruits more SLX4 to telomeres. The double-layered SLX4-TRF2 platform then assembles a nuclease toolkit at telomeres for HR-mediated telomere recombination, including T-SCE and t-loop resolution. Nuclease SLX1 catalyzes nucleolytic cleavage of telomere DNA and leads to "telomere trimming." We speculate that the telomere trimming process would continue until telomeres no longer bind sufficient TRF2 and hence the SLX4-SLX1 complex. We propose that SLX4-TRF2-assembled nuclease toolkit helps maintain an average equilibrium telomere length thus preventing telomere overlengthening. Our study reveals a major difference between TRF1 and TRF2 *cis*-acting mechanisms of telomere length regulation. Although TRF1 regulates telomere length via inhibiting telomerase activity, TRF2 recruits endonucleases via SLX4 to regulate telomere length. Because SLX4-TRF2-dependent telomere shortening occurs in both HeLa1.2.11 and ALT cells, nucleolytic cleavage of telomere DNAs by the SLX4-nuclease complex may be one of the common telomere length homeostasis mechanisms employed at long telomeres.

EXPERIMENTAL PROCEDURES

Protein Expression, Purification, Crystallization, and Structure Determination

Proteins were expressed in *E. coli* BL21(DE3) or B834(DE3). Human $TRF2_{TRFH}$ (residues 42–245), $TRF1_{TRFH}$ (residues 65–267), and $SLX4_{TBM}$ (residues 1014–1028), were purified by Ni-NTA (QIAGEN) metal affinity, followed by gel-filtration chromatography. The $SLX1_{WT\ or\ E82A}$-$SLX4_{SBR}$ complexes were purified by tandem affinity steps (Ni-NTA and glutathione Sepharose), followed by gel filtration. Crystals of the $SLX4_{TBM}$-$TRF2_{TRFH}$ complex were grown by sitting-drop vapor diffusion at 4°C. Structure of the $TRF2_{TRFH}$-$SLX4_{TBM}$ complex was solved by molecular replacement.

Telomere Detection Assays

Q-FISH (Zijlmans et al., 1997) or CO-FISH (Bailey et al., 2004) were used to measure telomere length and T-SCE, respectively. For IF-telomere FISH, cells were stained with primary and subsequently Alexa-Fluor-labeled secondary antibodies, followed by fixation and telomere-FISH (Wang et al., 2010). TCA (Zellinger et al., 2007) was used to detect telomere circles. Plasmid (Verdun and Karlseder, 2006) or oligonucleotide-based (Opresko et al., 2004) assays were used to detect D-loop resolution.

For additional details, see the Extended Experimental Procedures.

ACCESSION NUMBERS

Coordinates and structure factor amplitudes of the $SLX4_{TBM}$-$TRF2_{TRF}$ complex have been deposited in the Protein Data Bank under ID code 4M7C.

SUPPLEMENTAL INFORMATION

Supplemental Information includes Extended Results, Extended Experimental Procedures, five figures, and one table and can be found with this article online at http://dx.doi.org/10.1016/j.celrep.2013.08.017.

REFERENCES

Ancelin, K., Brunori, M., Bauwens, S., Koering, C.E., Brun, C., Ricoul, M., Pommier, J.P., Sabatier, L., and Gilson, E. (2002). Targeting assay to study the cis functions of human telomeric proteins: evidence for inhibition of telomerase by TRF1 and for activation of telomere degradation by TRF2. Mol. Cell. Biol. 22, 3474–3487.

Bailey, S.M., Goodwin, E.H., and Cornforth, M.N. (2004). Strand-specific fluorescence in situ hybridization: the CO-FISH family. Cytogenet. Genome Res. 107, 14–17.

Bianchi, A., and Shore, D. (2008). How telomerase reaches its end: mechanism of telomerase regulation by the telomeric complex. Mol. Cell 31, 153–165.

Blackburn, E.H. (2001). Switching and signaling at the telomere. Cell 106, 661–673.

Cesare, A.J., and Reddel, R.R. (2010). Alternative lengthening of telomeres: models, mechanisms and implications. Nat. Rev. Genet. 11, 319–330.

Chen, Y., Yang, Y., van Overbeek, M., Donigian, J.R., Baciu, P., de Lange, T., and Lei, M. (2008). A shared docking motif in TRF1 and TRF2 used for differential recruitment of telomeric proteins. Science 319, 1092–1096.

Fekairi, S., Scaglione, S., Chahwan, C., Taylor, E.R., Tissier, A., Coulon, S., Dong, M.Q., Ruse, C., Yates, J.R., 3rd, Russell, P., et al. (2009). Human SLX4 is a Holliday junction resolvase subunit that binds multiple DNA repair/recombination endonucleases. Cell 138, 78–89.

Griffith, J.D., Comeau, L., Rosenfield, S., Stansel, R.M., Bianchi, A., Moss, H., and de Lange, T. (1999). Mammalian telomeres end in a large duplex loop. Cell 97, 503–514.

Henson, J.D., and Reddel, R.R. (2010). Assaying and investigating Alternative Lengthening of Telomeres activity in human cells and cancers. FEBS Lett. 584, 3800–3811.

Kim, Y., Spitz, G.S., Veturi, U., Lach, F.P., Auerbach, A.D., and Smogorzewska, A. (2013). Regulation of multiple DNA repair pathways by the Fanconi anemia protein SLX4. Blood 121, 54–63.

Li, B., Oestreich, S., and de Lange, T. (2000). Identification of human Rap1: implications for telomere evolution. Cell 101, 471–483.

Muñoz, I.M., Hain, K., Déclais, A.C., Gardiner, M., Toh, G.W., Sanchez-Pulido, L., Heuckmann, J.M., Toth, R., Macartney, T., Eppink, B., et al. (2009). Coordination of structure-specific nucleases by human SLX4/BTBD12 is required for DNA repair. Mol. Cell 35, 116–127.

Opresko, P.L., Otterlei, M., Graakjaer, J., Bruheim, P., Dawut, L., Kølvraa, S., May, A., Seidman, M.M., and Bohr, V.A. (2004). The Werner syndrome helicase and exonuclease cooperate to resolve telomeric D loops in a manner regulated by TRF1 and TRF2. Mol. Cell 14, 763–774.

Palm, W., and de Lange, T. (2008). How shelterin protects mammalian telomeres. Annu. Rev. Genet. 42, 301–334.

Pickett, H.A., Cesare, A.J., Johnston, R.L., Neumann, A.A., and Reddel, R.R. (2009). Control of telomere length by a trimming mechanism that involves generation of t-circles. EMBO J. 28, 799–809.

Pickett, H.A., Henson, J.D., Au, A.Y., Neumann, A.A., and Reddel, R.R. (2011). Normal mammalian cells negatively regulate telomere length by telomere trimming. Hum. Mol. Genet. 20, 4684–4692.

Smogorzewska, A., van Steensel, B., Bianchi, A., Oelmann, S., Schaefer, M.R., Schnapp, G., and de Lange, T. (2000). Control of human telomere length by TRF1 and TRF2. Mol. Cell. Biol. 20, 1659–1668.

Svendsen, J.M., Smogorzewska, A., Sowa, M.E., O'Connell, B.C., Gygi, S.P., Elledge, S.J., and Harper, J.W. (2009). Mammalian BTBD12/SLX4 assembles a Holliday junction resolvase and is required for DNA repair. Cell 138, 63–77.

van Steensel, B., and de Lange, T. (1997). Control of telomere length by the human telomeric protein TRF1. Nature 385, 740–743.

Verdun, R.E., and Karlseder, J. (2006). The DNA damage machinery and homologous recombination pathway act consecutively to protect human telomeres. Cell 127, 709–720.

Wang, R.C., Smogorzewska, A., and de Lange, T. (2004). Homologous recombination generates T-loop-sized deletions at human telomeres. Cell 119, 355–368.

Wang, Z., Rhee, D.B., Lu, J., Bohr, C.T., Zhou, F., Vallabhaneni, H., de Souza-Pinto, N.C., and Liu, Y. (2010). Characterization of oxidative guanine damage and repair in mammalian telomeres. PLoS Genet. 6, e1000951.

Zellinger, B., Akimcheva, S., Puizina, J., Schirato, M., and Riha, K. (2007). Ku suppresses formation of telomeric circles and alternative telomere lengthening in Arabidopsis. Mol. Cell 27, 163–169.

Zeng, S., Xiang, T., Pandita, T.K., Gonzalez-Suarez, I., Gonzalo, S., Harris, C.C., and Yang, Q. (2009). Telomere recombination requires the MUS81 endonuclease. Nat. Cell Biol. 11, 616–623.

Zijlmans, J.M., Martens, U.M., Poon, S.S., Raap, A.K., Tanke, H.J., Ward, R.K., and Lansdorp, P.M. (1997). Telomeres in the mouse have large inter-chromosomal variations in the number of T2AG3 repeats. Proc. Natl. Acad. Sci. USA 94, 7423–7428.